

Efficient single-mode (TEM_{00}) Nd:YVO₄ laser with longitudinal 808-nm diode pumping

V.I. Donin, D.V. Yakovin, M.D. Yakovin

Abstract. A single-mode Nd:YVO₄ laser with unidirectional longitudinal pumping by laser diodes with $\lambda = 808$ nm and a power of 40 W is studied. In the TEM_{00} mode, the output laser power is 24 W with the optical efficiency $\eta_{opt} = 57.1\%$ (slope efficiency 63.3%), which, as far as we know, is the best result for Nd³⁺:YVO₄ lasers with longitudinal pumping at $\lambda = 808$ nm from one face of the active crystal. Estimates of thermal effects show that, using a Nd:YVO₄ crystal (length 20 mm, diameter 3 mm, dopant concentration 0.27 at%) with two undoped ends and bidirectional diode pumping with a total power of 170 W, one can obtain an output power of ~ 100 W in the TEM_{00} mode from one active element.

Keywords: diode-pumped laser, YVO₄/Nd:YVO₄ crystal, longitudinal pumping, thermal effects, high efficiency.

1. Introduction

At present, Nd:YAG and Nd:YVO₄ lasers with diode pumping at the wavelength $\lambda = 808$ nm have found wide application. Their optical efficiency (with respect to the pump diode power) η_{opt} in the multimode regime is rather high. For example, a Nd:YAG laser with an active rod 5 mm in diameter under the optimal conditions has $\eta_{opt} = 52.5\%$ and 54% upon transverse [1] and longitudinal [2] pumping at $\lambda = 808$ nm.

Most applications, such as precision processing of materials, pumping of harmonic generators and optical parametric oscillators, medicine, etc., require single-mode (TEM_{00}) operation. In the case of gas lasers with low concentrations of particles in the active media, for example, in high-power wide-aperture argon lasers, the TEM_{00} mode can be comparatively easily selected using V- or Z-shaped cavities with a large effective length (telescopic cavities) [3–5]*. However, the selection of the TEM_{00} mode in solid-state lasers runs into serious problems due to a high concentration of particles in the active media, which leads to thermo-optical distortions. In particular, according to [6], these distortions restrict the fundamental mode diameter approximately to 2 mm independently of the physical dimensions of the active rod. In addition, the ther-

* Unfortunately, formula (1) in [3] contains a misprint, namely, numeral 2 in front of R_3 in the denominator is absent, which was corrected in subsequent papers [4].

V.I. Donin, D.V. Yakovin, M.D. Yakovin Institute of Automation and Electrometry, Siberian Branch, Russian Academy of Sciences, prosp. Akad. Koptyuga 1, 630090 Novosibirsk, Russia; e-mail: donin@iae.nsk.su

Received 20 March 2013; revision received 7 May 2013
Kvantovaya Elektronika 43 (10) 903–906 (2013)
Translated by M.N. Basieva

mally induced internal stresses may cause breakdown of the crystal, which limits the output laser power. As a result, even for a laser with two Nd:YAG rods, the efficiency in the TEM_{00} mode regime does not exceed $\eta_{opt} = 18.9\%$ and 28% for transverse and longitudinal pumping, respectively [7, 8].

In this work, we study a single-mode Nd:YVO₄ laser with unidirectional pumping by laser diodes at $\lambda = 808$ nm with a power of 40 W. The output laser power in the TEM_{00} mode is 24 W with the optical efficiency $\eta_{opt} = 57.1\%$ (slope efficiency 63.3%). As far as we know, it is the highest power for lasers based on yttrium orthovanadate crystals with Nd³⁺ ions upon longitudinal pumping at $\lambda = 808$ nm from one face of the active crystal.

2. Experimental setup and main results

The scheme of the experimental setup is shown in Fig. 1. For pumping, we used an air-cooled diode laser (1) (Lumics, Germany) with ~ 40 -W unpolarised radiation at $\lambda = 808$ nm. The pump beam was coupled out through a fibre 400 μ m in diameter (NA = 0.22) and sent through a coupling system (2) to the entrance face of the active element.

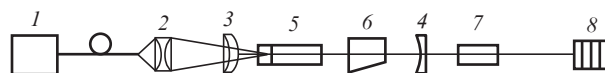


Figure 1. Scheme of the experimental setup: (1) fibre-coupled diode laser ($\lambda = 808$ nm); (2) optical coupling system; (3, 4) laser cavity mirrors; (5) YVO₄/Nd:YVO₄ active element; (6) acousto-optic modulator; (7) nonlinear crystal; (8) power meter.

The active element (5) was a diffusion-welded YVO₄/Nd:YVO₄ composite crystal of rectangular shape cut along the a crystallographic axis with dimensions $3 \times 3 \times 11$ mm. The face of the undoped part of the crystal with the length $l_n = 2$ mm was antireflection coated for the pump and laser wavelengths ($r_{808} < 2.5\%$ and $r_{1064} < 0.2\%$), and the exit face of the Nd³⁺-doped (0.27 at %) part with the length $l_d = 9$ mm was antireflection coated for the laser wavelength ($r_{1064} < 0.1\%$). The crystal was attached with heat conducting gaskets to a copper block, which was connected to an air cooling radiator through a Peltier element.

The coupling optical system (2) contained two lenses with focal lengths of 2.5 and 6 cm. The surfaces of the lenses were antireflection coated for $\lambda = 808$ nm ($r_{808} < 0.1\%$). The pump beam was focused by this system through the undoped end of the crystal on the surface of the doped part into a spot ~ 1 mm in diameter.

The laser cavity was formed by two mirrors: a meniscus mirror (3) with curvature radii of ± 500 mm ($r_{808} < 0.5\%$ on both faces and $r_{1064} > 99.7\%$ on the convex surface), through which the pump radiation was coupled in, and a spherical mirror (4) with a curvature radius 9600 mm and the transmission coefficient $\tau_{1064} = 20\%$. The active element was placed between the mirrors, at a distance of 15 mm from mirror (3). The total cavity length was varied from 75 to 280 mm.

For Q -switching, an acousto-optic modulator (6) was placed in the cavity. The maximum power of its controlling signal was 15 W (working frequency 80 MHz), which allowed us, if needed, to achieve laser pulses with a repetition rate of 50–100 kHz and a duration of 40–100 ns. To visualise the laser beam, we used the second harmonic generated in a non-linear crystal (7) placed outside the cavity (LBO, $4 \times 4 \times 18$ mm, type II synchronism, $\Theta = 22.5^\circ$). The output power of the laser and the pump diodes at the fibre exit was measured by a power meter (8) (Gentek, Canada).

The diode laser spectrum at the temperature $T = 23^\circ\text{C}$ is shown in Fig. 2. The pump radiation linewidth was 2.5 nm, which is close to the absorption linewidth of the Nd:YVO₄ active crystal [9]. The spectrum was measured using an MDR-23 monochromator with a 1200-lines mm^{-1} diffraction grating (instrumental width 0.13 nm).

The temperature distribution, the thermal lens parameters, and the internal stresses in the YVO₄/Nd:YVO₄ crystal were estimated using Comsol Multiphysics and MATLAB software packages. The steady-state temperature distribution

in the crystal was calculated by numerically solving the three-dimensional Poisson equation

$$K_x \frac{\partial^2 T(x, y, z)}{\partial x^2} + K_y \frac{\partial^2 T(x, y, z)}{\partial y^2} + K_z \frac{\partial^2 T(x, y, z)}{\partial z^2} + q(x, y, z) = 0, \quad (1)$$

where $q(x, y, z)$ is the absorbed pump power per unit volume; and K_x , K_y and K_z are the heat conductivities of the crystal along the x , y and z axes.

It was assumed that the $q(x, y, z)$ distribution is Gaussian,

$$q(x, y, z) = \frac{Q\alpha_\sigma \exp[-2(x^2 + y^2)/w_p^2 - \alpha_\sigma z]}{\pi w_p^2 [1 - \exp(-\alpha_\sigma l_d)]} + \frac{Q\alpha_\pi \exp[-2(x^2 + y^2)/w_p^2 - \alpha_\pi z]}{\pi w_p^2 [1 - \exp(-\alpha_\pi l_d)]}, \quad (2)$$

where $Q = P_{\text{in}}\eta$ is the thermal load determined by the pump power P_{in} and the quantum defect $\eta = 1 - \lambda_{808}/\lambda_{1064} = 1 - \eta_S$, α_σ and α_π are the absorption coefficients at $\lambda = 808$ nm for the σ - and π -polarisations, w_p is the pump beam waist on the face of the doped part of the crystal, and η_S is the Stokes factor.

The boundary conditions for Eqn (1) were as follows:

$$T(x = \pm b/2, y = \pm b/2) = T_0,$$

$$-K_z \frac{\partial T(x, y, z)}{\partial z} \Big|_{z = \pm(l_n + l_d)/2} = h\{T[z = \pm(l_n + l_d)/2] - T_a\}, \quad (3)$$

where b are the transverse dimensions of the crystal along the x and y axes; T_0 and T_a are the temperatures of the copper block and surrounding air, respectively; and h is the coefficient of convective heat transfer from the crystal faces. These boundary conditions mean that the exit and entrance faces of the crystal are cooled by convection and the temperature of the lateral surfaces is kept at T_0 ; the xyz coordinate system is positioned in the geometric centre of the crystal, and the z axis is directed along the a crystallographic axis.

In the calculations, we used the following parameters: $K_z = 5.23 \times 10^{-2} \text{ W cm}^{-1} \text{ K}^{-1}$, $K_x = K_y = 5.1 \times 10^{-2} \text{ W cm}^{-1} \text{ K}^{-1}$, $\alpha_\pi = 8.4 \text{ cm}^{-1}$, $\alpha_\sigma = 2.4 \text{ cm}^{-1}$, $P_{\text{in}} = 0\text{--}40 \text{ W}$, $\eta = 0.24$, $w_p = 5 \times 10^{-2} \text{ cm}$, $T_0 = T_a = 293 \text{ K}$ and $h = 2.5 \times 10^{-3} \text{ W cm}^{-2} \text{ K}^{-1}$.

To determine the thermal lens characteristics, we calculated the expression (optical path difference) [10]:

$$\text{OPD}(x, y) = \int_{-(l_n + l_d)/2}^{(l_n + l_d)/2} \left[\frac{\partial n}{\partial T} T(x, y) + \sum_{i,j=1}^3 \frac{\partial n}{\partial \varepsilon_{ij}} \varepsilon_{ij}(x, y) \right] dz + n_0 \Delta l(x, y), \quad (4)$$

where $\partial n/\partial T$ is the thermo-optical coefficient ($8.5 \times 10^{-6} \text{ K}^{-1}$); $\partial n/\partial \varepsilon_{ij}$ is the elasto-optic coefficient (which can be neglected for the Nd:YVO₄ crystal); ε_{ij} is the deformation tensor; n_0 is the refractive index at the temperature T_0 ;

$$\Delta l = \alpha_z \int_{-(l_n + l_d)/2}^{(l_n + l_d)/2} [T(x, y, z) - T(x = b/2, y = b/2, z = 0)] dz;$$

and $\alpha_z = 4.43 \times 10^{-6} \text{ K}^{-1}$ is the linear expansion coefficient along the a crystallographic axis. The lens focal length was estimated from the expression [10]

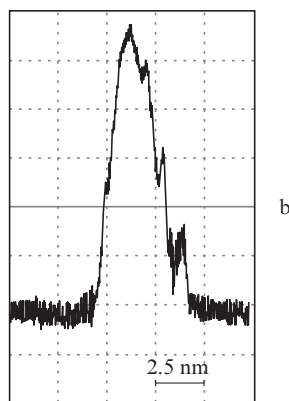
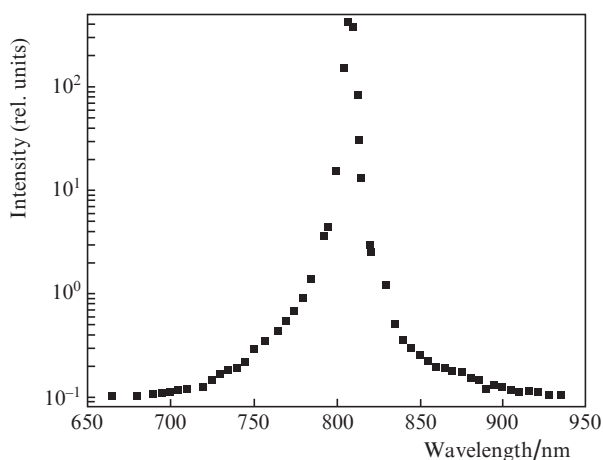


Figure 2. Diode laser spectrum in the region of 808 nm on (a) logarithmic and (b) linear scales.

$$f = b^2 / \{2[\text{OPD}_0 - \text{OPD}(x = b/2, y = b/2)]\}, \quad (5)$$

where $\text{OPD}_0 = \text{OPD}(x = 0, y = 0)$.

Our calculations show that, at a pump power of 40 W, the maximum calculated temperature difference along the longitudinal axis of the crystal is $\sim 140^\circ\text{C}$ (Fig. 3) and the focal length is $f \approx 200$ mm.

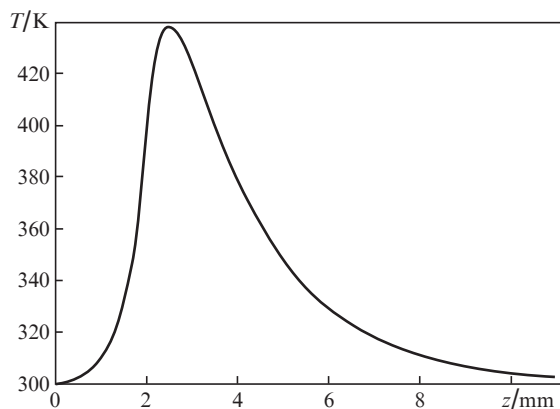


Figure 3. Calculated temperature distribution along the longitudinal axis of the crystal.

Figure 4 presents the dependence of the output laser power on the cavity length. With increasing length, the cavity approaches the stability edge and, at a critical length of ~ 280 mm, the cavity becomes unstable and lasing stops. The focal length of the thermal lens calculated from the critical cavity length is ~ 200 mm, which confirms the reliability of calculations. In this case, the calculated fundamental mode diameter is ~ 0.7 mm.

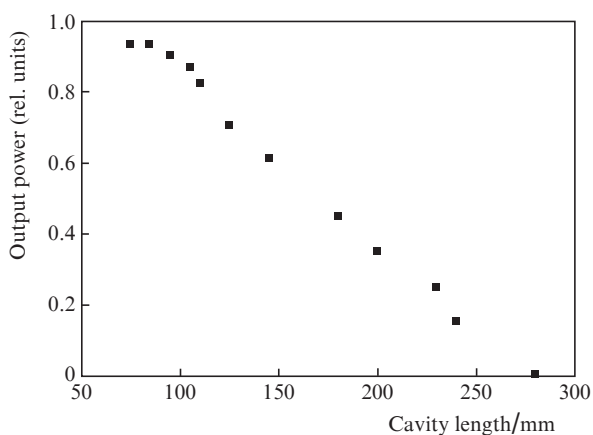


Figure 4. Dependence of the Nd:YVO₄ laser output power on the cavity length.

The dependence of the output laser power on the pump power is shown in Fig. 5. The maximum output power in the single-mode regime is 24 W at a pump power of 42 W and a lasing threshold of 2.1 W. The presented dependence is linear with a slope efficiency of 63.3%. The optical efficiency of the laser is $\eta_{\text{opt}} = 57.1\%$. With respect to the absorbed pump power (about 5% of pump power leaves the crystal), the slope and optical efficiencies are 66.6% and 60%, respectively.

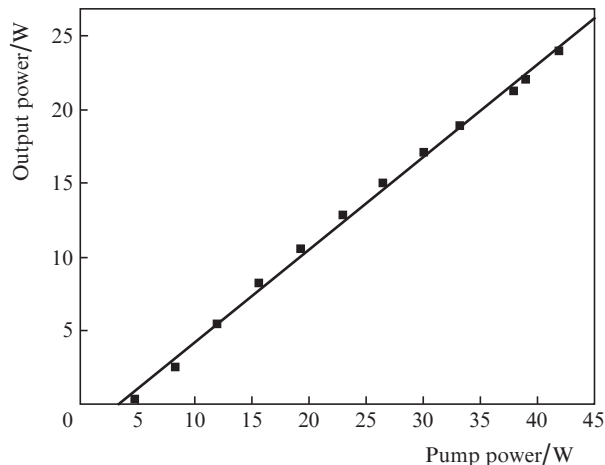


Figure 5. Output power of the Nd:YVO₄ laser as a function of the diode pump power.

3. Discussion of results

As was noted above, the main problem of high-power solid-state lasers is significant temperature gradients, which lead to unwanted thermo-optical effects. One can expect that the temperature gradients can be decreased by using pumping at longer wavelengths [11, 12]. In the case of pumping by laser diodes with $\lambda = 888$ or 914 nm instead of $\lambda = 808$ nm, the thermal load with respect to the pump power decreases from 24% to 17% and 14%, respectively, due to a change in the Stokes factor. However, this method has some drawbacks. First, due to low absorption coefficients at these pump wavelengths, a part of power is lost. For example, upon pumping at $\lambda = 914$ nm, these losses for our crystal are $\sim 90\%$. The absorption coefficient can be increased by using active media with larger concentrations of Nd^{3+} . Unfortunately, an increase in the Nd^{3+} concentration above 1% causes concentration quenching, which decreases the laser efficiency and increases the thermal load. Second, an increase in the pump power causes up-conversion, which also leads to these negative effects. The joint action of quenching and up-conversion was considered in [12], which showed their negative effect on laser operation in the Q -switching or amplifying regimes. In this connection, note that, at a random detuning of a high-power laser cavity in an ordinary regime, the mentioned effects also can sharply increase the heat release and cause breakdown of the active element.

Another important problem is the thermal stresses in the active crystal, which can lead to its breakdown. The stress σ_{max} , at which breakdown of Nd:YVO₄ crystals begins, is 53 MPa [9]. For a cylindrical rod upon longitudinal pumping, the expression for thermal stresses derived in [13] has the form

$$\sigma = \alpha E \frac{P_{\text{in}} \chi}{4\pi K} \frac{\alpha_p}{1 - \exp(-\alpha_p l)} \left\{ 1 - \frac{1}{2} \left[\frac{w_p(z)}{r_0} \right]^2 \right\}, \quad (6)$$

where α is the linear expansion coefficient, E is the Young modulus, α_p is the pump absorption coefficient ($\alpha_p \approx \alpha_\sigma/2 + \alpha_\pi/2$), l is the crystal length ($l = l_d$), K is the heat conductivity, χ is the fraction of absorbed power, and r_0 is the crystal radius. This expression shows that, at given power P_{in} and pump wavelength, the thermal loads can be decreased by decreasing α_p or r_0 , as well as by increasing w_p . Compared to [13], the temperature gradients in our composite crystal were decreased

(approximately by 1.5 times) with a corresponding decrease in σ . According to estimates obtained by formula (6), our composite crystal can withstand a pump power of ~ 70 W ($\sigma < \sigma_{\max}$), which gives hope for achieving an output laser power of ~ 40 W in the considered configuration (unidirectional pumping, $\lambda = 808$ nm).

In addition, calculations by formula (6) show that, in the case of one YVO₄/Nd:YVO₄ crystal with two undoped ends, ($l = 20$ mm, $r_0 = 1.5$ mm, $2 \times l_n = 4$ mm) and bidirectional diode pumping ($w_p = 1$ mm) at $\lambda = 808$ nm with the total power 2×85 W = 170 W, it is possible to reach a 100-W laser power in the TEM₀₀ mode. The Nd³⁺ concentration was taken to be 0.27 at %, the same as in our case. The thermal stresses in such a crystal are $\sim 0.8\sigma_{\max}$, while the temperature difference along the longitudinal axis of the crystal is $\sim 170^\circ\text{C}$.

Let us dwell on the issue of the TEM₀₀ mode selection. In addition to the obvious main factor – close diameters of the longitudinal pump and fundamental mode beams – note the following. Under our conditions, it was reasonable to expect absorption in the active crystal at $\lambda = 1064$ nm outside the pumped region due to the phonon population of the lower laser level from the Stark sublevels of the ground level. To verify this assumption, we performed a special experiment to detect this absorption.

Figure 6 shows the temperature dependence of the absorption of the π -polarised laser radiation in the studied crystal placed in a thermostat. This dependence was obtained by direct measurements of the absorption of attenuated radiation of a Nd:YAG laser with transverse pumping (linewidth 180 GHz) [14]. The absorption at $T = 20^\circ\text{C}$ was taken to be zero. The temperature shifts and temperature broadenings of lines in active elements were taken from [15] and [16], respectively. The observed absorption leads to additional losses outside the pumped region of the crystal (for nonaxial modes), which, as well as the mode competition, is favourable for single-mode lasing upon high-power longitudinal pumping. Thus, the observed temperature effect plays a positive role.

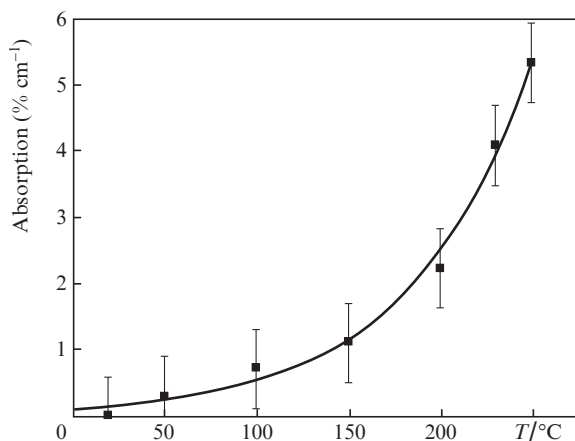


Figure 6. Absorption of π -polarised radiation with $\lambda = 1064$ nm in a Nd:YVO₄ crystal as a function of the crystal temperature.

4. Conclusions

An air-cooled single-mode laser with unidirectional 40-W pumping and an output power of 24 W is created for the first time. The laser has high slope (63.3%) and optical ($\eta_{\text{opt}} = 57.1\%$)

efficiencies. Our estimates of the thermal effects show that, from one YVO₄/Nd:YVO₄ crystal ($l = 20$ mm, $r_0 = 1.5$ mm, Nd³⁺ concentration 0.27 at%) under bidirectional diode pumping with a total power of 170 W at $\lambda = 808$ nm, it is possible to obtain a laser power of 100 W in the TEM₀₀ mode.

References

1. Qi Y., Zhu X., Lou Q., et al. *Opt. Express*, **13**, 8725 (2005).
2. Kracht D., Wilhelm R., Fredeet M., et al. *Opt. Express*, **13**, 10140 (2005).
3. Alferov G.N., Grigor'ev V.A., Donin V.I. *Kvantovaya Elektron.*, **5** (1), 29 (1978) [*Sov. J. Quantum Electron.*, **8** (1), 12 (1978)].
4. Donin V.I. *Moshchnye ionnye gasovye lasery* (High-Power Ion Gas Lasers) (Novosibirsk: Nauka, 1991).
5. Anan'ev Yu.A., Belousova I.M., Danilov O.B., Spiridonov V.V., Trofimov N.P. *Kvantovaya Elektron.*, **1** (2), 296 (1974) [*Sov. J. Quantum Electron.*, **4** (2), 164 (1974)].
6. Murdough M.P., Denman C.A. *Appl. Opt.*, **35**, 5925 (1996).
7. Hirano Y., Koyata Y., Yamamoto S., et al. *Opt. Lett.*, **24**, 679 (1999).
8. Frede M., Wilhelm R., Brendel M., et al. *Opt. Express*, **12**, 3581 (2004).
9. Koechner W. *Solid-State Laser Engineering* (New York: Springer Science and Business Media Inc., 2006).
10. Xiong Z., Li Zhigang G., Moore N., et al. *IEEE J. Quantum Electron.*, **39**, 979 (2003).
11. McDonagh L., Wallenstein R., Knappe R., Nebel A. *Opt. Lett.*, **31**, 3297 (2006).
12. Delen X., Balembois F., Musset O., Georges P. *J. Opt. Soc. Am. B*, **28**, 52 (2011).
13. Chen Y.F. *IEEE J. Quantum Electron.*, **35**, 234 (1999).
14. Donin V.I., Nikonov A.V., Yakovin D.V. *Kvantovaya Elektron.*, **34** (10), 930 (2004) [*Quantum Electron.*, **34** (10), 930 (2004)].
15. Delen X., Balembois F., Georges P. *J. Opt. Soc. Am. B*, **28**, 972 (2011).
16. Kaminskii A.A., Bogomolova G.A., Li L. *Izv. Akad. Nauk SSSR. Ser. Neorg. Mater.*, **5**, 673 (1969).